Upper bounds on coarsening rates

ROBERT V. KOHN

Courant Institute
New York University
251 Mercer Street
New York, NY 10012
kohn@cims.nyu.edu

and

FELIX OTTO

Institut für Angewndte Mathematik
Universität Bonn
Wegelerstr. 10
53115 Bonn, Germany
otto@iam.uni-bonn.de

Abstract. We consider two standard models of surface-energy-driven coarsening: a constant-mobility Cahn-Hilliard equation, whose large-time behavior corresponds to Mullins-Sekerka dynamics; and a degenerate-mobility Cahn-Hilliard equation, whose large-time behavior corresponds to motion by surface diffusion. Arguments based on scaling suggest that the typical length scale should behave as $\ell(t) \sim t^{1/3}$ in the first case and $\ell(t) \sim t^{1/4}$ in the second. We prove a weak, one-sided version of this assertion — showing, roughly speaking, that no solution can coarsen faster than the expected rate. Our result constrains the behavior in a time-averaged sense rather than pointwise in time, and it constrains not the physical length scale but rather the perimeter per unit volume. The argument is simple and robust, combining the basic dissipation relations with an interpolation inequality and an ODE argument.

Key words and phrases: coarsening, Cahn-Hilliard, Mullins-Sekerka, surface diffusion

1 Introduction

We prove rigorous upper bounds on the coarsening rates for two standard models of surface-energy-driven interfacial dynamics. The sharp-interface versions of these models are the Mullins-Sekerka law (MS) and motion by surface diffusion (SD). Both evolutions preserve volume and decrease surface energy. The difference between them lies in the mechanism of rearrangement: MS corresponds to diffusion through the bulk, while SD corresponds to diffusion along the interfacial layer.

We prefer to work with diffuse-interface versions of these models. Therefore rather than analyze the sharp-interface MS and SD laws, we shall consider two Cahn-Hilliard equations — one with constant mobility, the other with degenerate mobility

— whose large-time regimes are described by MS and SD respectively. We prefer the Cahn-Hilliard models because they make sense even when the geometry becomes singular, for example due to a topological transition such as pinch-off. The Cahn-Hilliard viewpoint is also attractive because it can be derived from a stochastic Ising model, and because it provides a unified description of spinodal decomposition and coarsening.

Our focus is the large-time coarsening behavior, i.e. the growth of the characteristic length scale $\ell(t)$ as $t \to \infty$. The expected behavior is

$$\ell(t) \sim t^{1/3} \text{ for Mullins-Sekerka}, \quad \ell(t) \sim t^{1/4} \text{ for surface diffusion.} \tag{1}$$

To explain why, recall that both MS and SD are *scale-invariant*: solutions of MS are preserved by $x \to \lambda x$, $t \to \lambda^3 t$, while those of SD are preserved by $x \to \lambda x$, $t \to \lambda^4 t$. Thus if there is any universal law for ℓ it must be given by (1).

In truth, much more than (1) is conjectured: solutions with random initial data are believed to be *statistically self-similar*. Such behavior has been confirmed by numerical and physical experiments, but we know no rigorous results in this direction.

The proposed coarsening law (1) can be decomposed into two rather different assertions:

(a) an upper bound for $\ell(t)$, saying that microstructure cannot coarsen faster than the similarity rate; and

(b) a lower bound for $\ell(t)$, saying that microstructure must coarsen at least at the similarity rate.

Assertion (b) is subtle: it may be true generically, or with probability one — but viewed as a universal statement it is clearly false, since there are configurations that do not coarsen at all (e.g. parallel planar layers). We have nothing new to say about it.

Assertion (a) is however different and easier, because it should be true universally. Therefore it can be approached using deterministic methods. That is the goal of the present paper. Our main achievement is a (very) weak version of (a). It constrains the behavior in a time-averaged sense rather than pointwise in time, and it constrains not the physical length scale but rather the surface energy per unit volume.

Our approach is relatively simple and robust. We outline it here using the language of the sharp-interface models, though the proofs presented later are for the Cahn-Hilliard equations. The argument makes use of *interfacial energy density*

$$E(t) = \text{ interfacial area per unit volume,}$$

which has the dimensions of 1/length, and the *physical scale*

$$L(t) = \text{ a suitable negative norm of the order parameter}$$

which has dimensions of length. They are related by a sort of *interpolation inequality* — a basic fact of analysis, having nothing to do with the dynamics — which says

$$EL \geq C \tag{2}$$

for some positive universal constant C. Of course the interfacial area decreases, in other words

$$\dot{E} \leq 0, \tag{3}$$

since the motion is surface-energy-driven. In addition — this is the heart of the matter — we also have differential inequalities

$$
\begin{array}{rcll}
(\dot{L})^2 & \leq & C\,(-\dot{E}) & \text{for MS} \\
(\dot{L})^2 & \leq & C\,E\,(-\dot{E}) & \text{for SD}
\end{array}
\tag{4}
$$

as consequences of the basic energy-dissipating structure of the dynamics. Our upper bound on the time-averaged coarsening rate follows from these relations by an elementary ODE argument. The main conclusion is

$$
\begin{array}{rcll}
\frac{1}{T}\int_0^T E^2\,dt & \geq & C\frac{1}{T}\int_0^T (t^{-\frac{1}{3}})^2 & \text{for MS} \\
\frac{1}{T}\int_0^T E^3\,dt & \geq & C\frac{1}{T}\int_0^T (t^{-\frac{1}{4}})^3 & \text{for SD}
\end{array}
$$

for $T \gg 1$. This is a time-averaged version of the (unproved) pointwise statement

$$
\begin{array}{rcll}
E^{-1} & \leq & Ct^{1/3} & \text{for MS} \\
E^{-1} & \leq & Ct^{1/4} & \text{for SD,}
\end{array}
$$

which is in turn a one-sided version of (1) with $\ell = E^{-1}$.

We emphasize that bounding the coarsening rate from above is quite different from bounding it from below. Our upper bound is a matter of kinematics, while a lower bound would be a matter of geometry. Indeed, a system cannot coarsen too quickly, no matter how large its curvature, due to the kinematic restrictions (2)-(4); it can however coarsen slowly if its curvature is small. The situation is roughly analogous to the blowup of semilinear heat equations, where local-in-time existence theory gives a lower bound on the blowup rate but faster blowup is possible, see e.g. [16, 19]. Another analogy is to diffusion-enhanced convection of active scalars, where kinematic considerations lead to upper but not lower bounds for the effective diffusivity, see e.g. [8].

We need a scheme for spatial averaging, to define the quantities E and L, and to prove the fundamental relations (2)-(4). Our choice is to consider solutions that are *spatially periodic*. This does not significantly compromise the physics, since the size of the period cell and the complexity of the initial data are unrestricted. The constants in our estimates are of course independent of the period cell.

We shall focus on the case of a "critical mixture," i.e. the two phases are assumed to have equal volume fractions. This simplifies the notation somewhat, and it is

physically natural when the mixture originates from spinodal decomposition. The restriction of equal volume fractions is, however, merely a convenience, not a mathematical necessity. Similar results hold, with similar proofs, at any volume fraction.

Our rigorous analysis is restricted to the diffuse-interface (Cahn-Hilliard) setting. However, a similar analysis can be given for "reasonable" solutions of the sharp-interface evolution laws — for example, solutions which are classical at all but finitely many times, and continuous across the singular times.

The paper is organized as follows. Section 2 provides physical and mathematical background concerning the Cahn-Hilliard and sharp-interface models. Section 3 states our rigorous results on the coarsening rate, and Section 4 presents the proofs. Section 5 concludes with a brief discussion.

2   Background

We have been discussing four evolutions: the sharp-interface MS and SD laws, and the diffuse-interface Cahn-Hilliard equations associated with them. There is, however, a natural unity to the story: all four evolutions arise as limits of a single equation, with a clear link to stochastic Ising models. Sections 2.1 and 2.2 present this unifying viewpoint, and explain how it leads to our two Cahn-Hilliard models — with constant vs. degenerate mobility — in the shallow-quench vs. deep-quench regimes. Section 2.3 discusses the large-time behavior of these Cahn-Hilliard models, explaining their connection with the sharp-interface MS and SD laws. Finally Section 2.4 discusses the scale-invariance of the sharp-interface laws, and the associated conjectures about their coarsening behavior. None of this material is strictly necessary to understand our rigorous analysis: the impatient reader can skip straight to Section 3.

2.1   A unifying Cahn-Hilliard model: variable quench

Our starting point is the following Cahn-Hilliard-type model. The free energy is given by

$$E = \fint \left\{ \frac{\beta}{2} \left(|\nabla m|^2 + (1 - m^2) \right) + \frac{1}{2} \left((1+m)\log(1+m) + (1-m)\log(1-m) \right) \right\} dx, \tag{5}$$

where $m \in (-1, 1)$. Here $c = \frac{1}{2}(1 + m) \in (0, 1)$ stands for the relative concentration of, say, the first species. We have normalized the total free energy by the volume of the system, denoting the average by $\fint$. The first term in (5) is of enthalpic, the second term of entropic origin; β is the inverse temperature. The relative concentration evolves to reduce E while preserving the volume of each phase:

$$\frac{\partial m}{\partial t} - \nabla \cdot \left((1 - m^2) \nabla \frac{\partial E}{\partial m} \right) = 0, \tag{6}$$

which leads to the equation

$$\frac{\partial m}{\partial t} - \nabla^2 m + \beta \, \nabla \cdot \left((1 - m^2) \, \nabla (m + \nabla^2 m) \right) \;=\; 0. \tag{7}$$

We will be interested in the case of a "critical mixture", in other words one with

$$\fint m \, dx \;=\; 0. \tag{8}$$

This model (7) is a natural starting point, because it has a firm microscopic foundation: it is a local version of the macroscopic limit of an Ising model with long-range Kac potential and Kawasaki dynamics; see [15] or the review article [14, Theorem 6.1]. In particular, the specific form of the mobility $1 - m^2$ in (6), which vanishes at the two extreme values $m = \pm 1$, is natural.

It is well-known and easy to verify that for $\beta > 1$, (5) has two bulk equilibrium values, $m_+ \in (0, 1)$ and $m_- = -m_+$. They behave as

$$m_+ \;\approx\; \left\{ \begin{array}{ll} (3 \, (\beta - 1))^{\frac{1}{2}} & \text{for } 0 < \beta - 1 \ll 1 \\ 1 - 2 \, \exp(-2 \, \beta) & \text{for } \beta \gg 1 \end{array} \right\}.$$

Hence one is lead to consider two regimes, the "shallow quench" $0 < \beta - 1 \ll 1$ and the "deep quench" $\beta \gg 1$.

2.2 Shallow and deep quench regimes: constant vs. degenerate mobility

In the shallow quench regime, it is natural to rescale time, space, concentration and energy according to

$$t \;=\; \left(\frac{2}{\beta - 1} \right)^2 \hat{t}, \qquad x \;=\; \left(\frac{2}{\beta - 1} \right)^{\frac{1}{2}} \hat{x},$$

$$m \;=\; (3 \, (\beta - 1))^{\frac{1}{2}} \, \hat{m}, \qquad E \;=\; \frac{3}{2} \, (\beta - 1)^2 \, \hat{E} + \text{const.}$$

As $\beta \to 1$ the bulk equilibrium values become

$$\hat{m}_\pm \;=\; \pm 1$$

and equations (5) and (6) become (formally, to leading order)

$$\hat{E} \;=\; \fint \frac{1}{2} \left(|\nabla \hat{m}|^2 + (1 - \hat{m}^2)^2 \right) \, d\hat{x} \tag{9}$$

and

$$\frac{\partial \hat{m}}{\partial \hat{t}} - \hat{\nabla}^2 \frac{\partial \hat{E}}{\partial \hat{m}} \;=\; 0,$$

yielding the Cahn-Hilliard equation with constant mobility

$$\frac{\partial \hat{m}}{\partial \hat{t}} + \hat{\nabla}^2 \left(\hat{\nabla}^2 \hat{m} + 2\left(1 - \hat{m}^2\right)\hat{m} \right) \;=\; 0. \tag{10}$$

This is the Cahn-Hilliard equation associated with MS dynamics, as we shall explain presently.

The deep quench regime is even more obvious: One rescales time and energy according to

$$t \;=\; \frac{1}{\beta}\,\hat{t}, \quad E \;=\; \beta\,\hat{E} \;+\; \text{const},$$

and obtains formally from (5) and (6) to leading order

$$\hat{E} \;=\; \oint \frac{1}{2}\left(|\nabla m|^2 + (1 - m^2) \right)\,dx$$

resp.

$$\frac{\partial m}{\partial \hat{t}} - \nabla \cdot \left[(1 - m^2)\,\nabla \frac{\partial \hat{E}}{\partial m} \right] \;=\; 0,$$

yielding the Cahn-Hilliard equation with degenerate mobility

$$\frac{\partial m}{\partial \hat{t}} + \nabla \cdot \left[(1 - m^2)\,\nabla\left(\nabla^2 m + m \right) \right] \;=\; 0. \tag{11}$$

This is the Cahn-Hilliard equation associated with SD dynamics, as we shall explain below. The preceding argument, deriving (11) as the deep-quench limit of (7), has been made rigorous by Elliott & Garcke [9].

Our attention in the remainder of this paper will be restricted to the two Cahn-Hilliard equations (10) and (11). We shall of course drop the hats. We remark that these Cahn-Hilliard equations, being fourth-order, have no maximum principle. However, solutions of (11) preserve the constraint $-1 \leq m \leq 1$, as a consequence of the degenerate mobility $1 - m^2$, which vanishes at the bulk equilibrium values $m = \pm 1$ [9].

2.3 The interfacial regime

Experimental observation and numerical simulation shows the following scenario (see e.g. [11, 12, 28]). Consider as initial data the uniform critical mixture $m = 0$, which is an unstable equilibrium of E, perturbed by some stationary random fluctuations of amplitude $o(1)$ and correlation length $o(1)$. The linearization selects a most unstable wavelength, which in our non-dimensionalization is $O(1)$; fluctuations of this wavelength grow fastest.

After this exponential growth regime, nonlinear effects kick in: m approximately saturates at its bulk equilibrium values ± 1 in most of the sample. The order parameter m attains its bulk equilibrium value 1 in a convoluted region of characteristic

length scale $\ell \gg 1$. Likewise, there is a region where m attains the other bulk equilibrium value. These regions represent distinct "phases," and their geometry is highly connected (a "bicontinuous" phase distribution). Each phase has volume fraction $1/2$, since the evolution preserves the constraint $\fint m = 0$. The phases are separated by a transition layer of width $O(1)$. The profile of m across the transition layer is approximately in equilibrium. Based on the explicit form of the equilibrium profile, one obtains for the energy E per unit volume

$$E \approx \left\{ \begin{array}{ll} \frac{4}{3}\,\text{interfacial area density} & \text{in the constant mobility case} \\[2mm] \frac{\pi}{2}\,\text{interfacial area density} & \text{in the degenerate mobility case} \end{array} \right\} \tag{12}$$

As the system matures it enters the "interfacial regime," characterized by small energy per unit volume and large characteristic length scale:

$$E \ll 1 \quad \text{and} \quad \ell \gg 1. \tag{13}$$

In this regime the evolution is essentially geometric, since the interface is sharp on the scale ℓ of the regions it separates. Motion is driven by the reduction of the total interfacial area, limited by diffusion through the bulk for the case of constant mobility resp. along the interface for the case of degenerate mobility. It leads to a coarsening of the phase distribution, that is, to an increase of its characteristic length scale ℓ.

The geometric evolution associated with our constant-mobility Cahn-Hilliard equation (10) is the Mullins-Sekerka law, which prescribes the normal velocity V of the evolving interface Γ as follows. First, let p be the chemical potential defined by

$$-\nabla^2 p = 0 \text{ outside } \Gamma, \quad p = \frac{1}{3} H \text{ on } \Gamma,$$

where H denotes the mean curvature. Then V is given by

$$V = [\frac{\partial p}{\partial \nu}] \text{ on } \Gamma, \tag{14}$$

where $[\frac{\partial p}{\partial \nu}]$ denotes the jump in the normal derivative $\frac{\partial p}{\partial \nu}$ of p across Γ. The fact that large-time Cahn-Hilliard coarsening is described by the Mullins-Sekerka regime was shown by Pego [27] using a formal, asymptotic-expansion-based argument (see [2] for the multicomponent case). A rigorous proof of this result was given by Alikakos, Bates & Chen, provided the limiting Mullins-Sekerka law has a smooth solution [1]. A rigorous result not requiring any regularity hypotheses, using a very weak notion of solution of the Mullins-Sekerka law, was given by Chen [4].

The geometric evolution associated with our degenerate-mobility Cahn-Hilliard equation (11) is motion by surface diffusion. It prescribes the normal velocity V of the evolving interface Γ by

$$V = -\frac{\pi^2}{16} \nabla_s^2 H \quad \text{on } \Gamma, \tag{15}$$

where ∇_s^2 denotes the surface Laplacian on Γ. This was shown by Cahn, Elliott & Novick-Cohen [3] using a formal, asymptotic-expansion-based argument (see also [13] for the multi component case). There is, to our knowledge, as yet no rigorous version of this result.

The literature on Cahn-Hilliard equations, sharp-interface limits, and related topics is vast; additional information and references can be found in the review [10].

2.4   Scaling

The sharp-interface models are important for their scale-invariance: solutions are preserved under the scaling

$$
\begin{array}{llll}
x = \lambda\,\hat{x}, & t = \lambda^3\,\hat{t} & \text{for Mullins-Sekerka} \\
x = \lambda\,\hat{x}, & t = \lambda^4\,\hat{t} & \text{for surface diffusion}
\end{array}
\tag{16}
$$

as an easy consequence of the definitions (14) and (15). Solutions of the Cahn-Hilliard equations are, therefore, approximately scale-invariant in the interfacial regime.

Of course we do not expect the phase geometry to be pointwise scale invariant. But for a critical mixture (one with $\fint m = 0$), numerical simulations suggest that solutions in the interfacial regime are *statistically self-similar* (see e.g. [11, 12, 28]). Such behavior imposes itself after an initial transient, and persists as long as the length scale ℓ of the phase distribution is much smaller than the system size — after which finite-size effects take over. Conceptually, statistical self-similarity means that the (suitably defined, random) solution is invariant under the scaling (16). Practically, we can replace statistical averaging by spatial averaging to derive the following very measurable consequence: the two-point correlation function $c(t, r)$ should have the form

$$
c(t, r) = \hat{c}(\frac{r}{\ell}) \quad \text{where} \quad \ell = t^\alpha,
\tag{17}
$$

for some universal profile $\hat{c}(r)$, with $\alpha = 1/3$ in the constant-mobility (MS) setting, and $\alpha = 1/4$ in the degenerate-mobility (SD) setting. Such self-similarity is indeed seen experimentally; for example it is a robust feature of many experiments in the spinodal decomposition of polymer melts, where the Fourier transform of the correlation function (the "structure factor") can be measured with high precision [18, 20].

To our knowledge, there is no convincing theoretical explanation for the observed statistical self-similarity. The closest thing we know to such an explanation is the mean-field theory of Ostwald ripening. This amounts to the constant-mobility Cahn Hilliard model (or the Mullins-Sekerka law) applied to a strongly off-critical mixture (volume fraction of one phase close to zero, i.e. $\fint m\,dx + 1 \ll 1$). In this setting, the minority phase $m \approx 1$ breaks into many nearly spherical droplets of varying

radius. The Lifshitz-Slyozov-Wagner mean field theory [21, 31] gives an evolution equation for the number density $f(t, R) \, dR$ of droplets of radius R at time t. This evolution equation has been given a rigorous justification [24, 25]. It admits self-similar solutions, which can be viewed as "statistically self-similar" configurations at the level of the distribution of radii. Surprisingly, however, the large-time behavior is *not* necessarily self-similar within this simple mean–field theory [26].

The conjecture (17), asserting self-similarity of the correlation functions, seems intractable. We therefore concentrate on the subsidiary, presumably easier conjecture that

$$\ell \, \sim \, t^\alpha$$

with α determined by scaling. Let us work out the plausible range of validity of this statement. Assume $t = 0$ corresponds to a fixed time where we are already in the interfacial regime, that is

$$E_0 \; := \; E(t = 0) \; \ll \; 1, \quad \ell_0 \; := \; \ell(t = 0) \; \gg \; 1. \tag{18}$$

In view of the scale invariance (16), we expect

$$\ell \, \sim \, \left\{ \begin{array}{llll} (t + \ell_0^3)^{\frac{1}{3}} & \sim & t^{\frac{1}{3}} & \text{for } t \gg \ell_0^3 \quad \text{constant mobility} \\ (t + \ell_0^4)^{\frac{1}{4}} & \sim & t^{\frac{1}{3}} & \text{for } t \gg \ell_0^4 \quad \text{degenerate mobility} \end{array} \right\}.$$

Because of (12), we expect that

$$E \, \sim \, \ell^{-1},$$

so the preceding relation becomes

$$E \, \sim \, \left\{ \begin{array}{lll} t^{-\frac{1}{3}} & \text{for } t \gg \ell_0^3 & \text{constant mobility} \\ t^{-\frac{1}{4}} & \text{for } t \gg \ell_0^4 & \text{degenerate mobility} \end{array} \right\}.$$

Thus, taking into account the hypothesis (18), we expect

$$E \, \sim \, \left\{ \begin{array}{lll} t^{-\frac{1}{3}} & \text{for } t \gg \ell_0^3 \gg 1 \gg E_0 & \text{constant mobility} \\ t^{-\frac{1}{4}} & \text{for } t \gg \ell_0^4 \gg 1 \gg E_0 & \text{degenerate mobility} \end{array} \right\}. \tag{19}$$

The main result of this paper is a one-sided, time-averaged version of (19).

3   The main result

The last two sections mixed rigorous statements with many heuristic arguments and conjectures. From here on, however, our treatment is fully rigorous. We consider solutions of the "constant-mobility" Cahn-Hilliard equation

$$\frac{\partial m}{\partial t} + \nabla^2 \left(\nabla^2 m + 2 \left(1 - m^2 \right) m \right) \; = \; 0 \quad \textit{constant mobility, Eqn. (10)}$$

with associated energy

$$E \;=\; \fint \frac{1}{2} \left(|\nabla m|^2 + (1 - m^2)^2 \right) dx;$$

and solutions of the "degenerate-mobility" Cahn-Hilliard equation

$$\frac{\partial m}{\partial t} + \nabla \cdot \left[(1 - m^2) \nabla \left(\nabla^2 m + m \right) \right] \;=\; 0 \quad \textit{degenerate mobility, Eqn. (11)}$$

with associated energy

$$E \;=\; \fint \frac{1}{2} \left(|\nabla m|^2 + (1 - m^2) \right) dx.$$

We restrict our attention for simplicity to the case of a critical mixture, i.e. to solutions with

$$\fint m \, dx \;=\; 0 \quad \textit{critical mixture, Eqn. (8).}$$

The initial value problem for the constant-mobility Cahn-Hilliard equation is well-posed and solutions are smooth. Less is known about the degenerate-mobility: weak solutions are known to exist [9] but uniqueness remains open. Our arguments are valid for the weak solutions constructed in [9].

We always use periodic boundary conditions for the PDE's, and $\fint$ denotes averaging over the period cell. The size Λ of the period cell is effectively the system size; the interesting case is $\Lambda \gg 1$. We always work with averages, so the system size Λ never enters our analysis. In particular, our upper bounds on the coarsening rate are independent of system size.

As a specific solution coarsens, its length scale must eventually approach the system size. When this happens finite-size effects will slow and eventually stop the coarsening. This behavior does not falsify our results, since we discuss only *upper* bounds on the coarsening rate.

Our analysis uses two different measures of the length scale of the microstructure. One is the interfacial energy density; we explained in Section 2.3 that E itself is a good proxy for this. The other is the physical scale — the quantity ℓ in our heuristic discussions. The convenient definition of this quantity is the following:

Definition 1 *For any spatially-periodic $m(x)$ with mean value zero, its physical scale $L = L[m]$ is*

$$L \;:=\; \fint |\nabla^{-1} m| \, dx \;:=\; \sup \left\{ \fint m \zeta \, dx \mid \textit{periodic } \zeta \textit{ with } \sup |\nabla \zeta| \le 1 \right\}. \qquad (20)$$

The notation $\fint |\nabla^{-1} m| \, dx$ is purely formal: it is not the L^1 norm of some function $\nabla^{-1} m$. Rather, it reminds us that $L[m]$ is dual to the $W^{1,\infty}$ norm on ζ. (To extend our analysis to off-critical mixtures, i.e. to permit $\fint m \ne 0$, one must restrict ζ in (20) to have mean value 0.)

We now state our main results. For maximum clarity we state a special case of our result as Theorem 1, then the general case as Theorem 2.

Theorem 1 *If the initial energy is E_0 and the initial length scale is L_0 then we have*

$$\fint_0^T E^2 dt \ \gtrsim \ \fint_0^T (t^{-\frac{1}{3}})^2 dt \quad \text{for } T \gg L_0^3 \gg 1 \gg E_0 \quad \text{constant mobility}$$

$$\fint_0^T E^3 dt \ \gtrsim \ \fint_0^T (t^{-\frac{1}{4}})^3 dt \quad \text{for } T \gg L_0^4 \gg 1 \gg E_0 \quad \text{degenerate mobility.}$$

Remark 1 *The detailed statement of Theorem 1 is this: There exists a (possibly large but controlled) universal constant $C < \infty$ (depending only on the space dimension N) such that*

$$\frac{1}{T} \int_0^T E^2 dt \ \geq \ \frac{1}{C} T^{-\frac{2}{3}} \quad \text{provided } T \geq C L_0^3 \ \text{and} \ E_0 \leq \frac{1}{C}$$

for the constant mobility case and a similar statement in the degenerate mobility case. Here and throughout, the symbols $\gtrsim$, $\gg$ resp. $\lesssim$ and $\ll$ bear precisely this meaning. The symbol $\sim$ means both $\gtrsim$ and $\lesssim$.

Theorem 1 asserts that $E \gtrsim t^{-1/3}$ in a suitable time-averaged sense for the case of constant mobility, and $E \gtrsim t^{-1/4}$ in a different time-averaged sense for the case of degenerate mobility. It is natural to ask whether similar bounds hold for other norms of E, and with E replaced by $E^\theta L^{-(1-\theta)}$. The answer is yes: the method used to prove Theorem 1 actually shows the following stronger result.

Theorem 2 *For any $0 \leq \theta \leq 1$, suppose r satisfies*

$$r < 3, \quad \theta r > 1 \quad \text{and} \quad (1-\theta)r < 2 \quad \text{in the case of constant mobility} \quad (21)$$
$$r < 4, \quad \theta r > 2 \quad \text{and} \quad (1-\theta)r < 2 \quad \text{in the case of degenerate mobility.} \quad (22)$$

Then we have

$$\fint_0^T E^{\theta r} L^{-(1-\theta)r} dt \ \gtrsim \ \fint_0^T (t^{-\frac{1}{3}})^r dt \quad \text{for } T \gg L_0^3 \gg 1 \gg E_0 \quad \text{constant mobility}$$

$$\fint_0^T E^{\theta r} L^{-(1-\theta)r} dt \ \gtrsim \ \fint_0^T (t^{-\frac{1}{4}})^r dt \quad \text{for } T \gg L_0^4 \gg 1 \gg E_0 \quad \text{degenerate mobility.}$$

The values of r and θ permitted by (21) and (22) are shown in Figure 1 resp. 2. Notice that when $\theta = 1$, (21) permits any $1 < r < 3$ and (22) permits any $2 < r < 4$. Also notice that the minimum possible θ permitted by (21) is $1/3$, while the minimum permitted by (22) is $1/2$. The conclusion of the theorem is strongest when θ and r are smallest, i.e. for values close to the curve $\theta r = 1$ (constant mobility) resp. $\theta r = 2$ (degenerate mobility). Indeed, focusing for simplicity on the constant mobility case, if the estimate holds for a given $r_0 < 3$ then it holds for all r between r_0 and 3 by an application of Jensen's inequality; and if the estimate holds for a given $\theta_0 < 1$ then it holds for all $\theta > \theta_0$ by an application of Lemma 1 below.
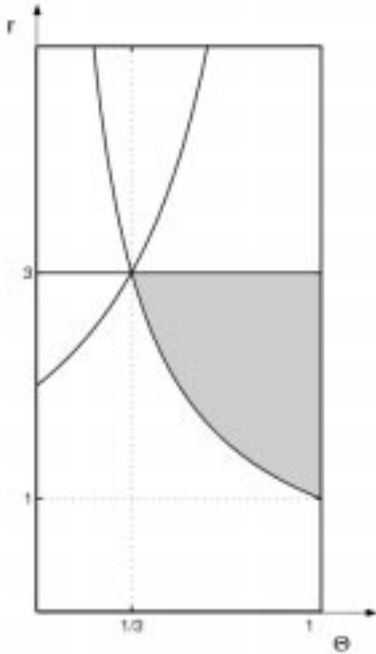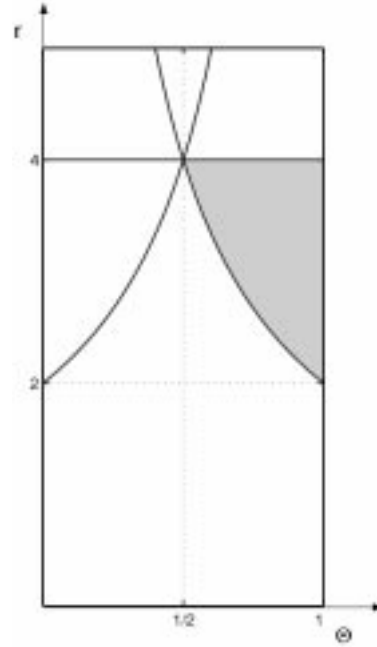
Fig. 1: constant mobility   Fig. 2: degenerate mobility

4   The proof

Theorems 1 and 2 are immediate consequences of three basic lemmas. We state them in Section 4.1, then prove each in turn in Sections 4.2-4.4.

4.1   Ingredients

The first basic lemma relates L and E using just their definitions — making no use of the Cahn-Hilliard dynamics. As motivation, we observe that L scales like length. In the interfacial regime $E \ll 1$, according to (12), E is essentially the interfacial area density, which scales like inverse length. So it is tempting to suggest that $E\,L \sim 1$. This is true for sufficiently simple geometries with a *single* length scale. In general, however, there is only an inequality:

Lemma 1 *(Interpolation)*

$$E\,L \stackrel{>}{\sim} 1 \quad for \quad E \ll 1.$$

We call this an "interpolation" lemma because it is closely related to the following relation, asserted for spatially periodic f with mean value 0:

$$\fint |f|\,dx \stackrel{<}{\sim} \left(\fint |\nabla f|\,dx \right)^{1/2} \left(\fint |\nabla^{-1} f|\,dx \right)^{1/2}. \tag{23}$$

The proof is similar to (but easier than) the one given below for Lemma 1. We obtain a geometric statement by choosing f to take only the values ± 1, so that

$\fint |f|\, dx = 1$ and $\fint |\nabla f|\, dx$ is twice the interfacial area density. Thus (23) contains a sharp-interface version of Lemma 1.

We note in passing that interpolation inequalities similar to (23) — interpolating between the BV norm $\fint |\nabla f|\, dx$ and a suitable negative norm — were central to our recent work with Choksi on domain branching in uniaxial ferromagnets [5]. Inequalities of this type have also emerged from recent work on nonlinear approximation theory [6, 7].

The second basic lemma restricts the rate at which L can change. In our Cahn-Hilliard models, the free energy E is dissipated by friction. The following lemma says that a change of the length scale L has to overcome significant friction, and is therefore accompanied by a significant reduction of the free energy E.

Lemma 2 *(Dissipation)*

$$
\begin{aligned}
(\dot{L})^2 &\lesssim & -\dot{E} && \text{\itshape constant mobility} \\
(\dot{L})^2 &\lesssim & E\,(-\dot{E}) && \text{\itshape degenerate mobility}
\end{aligned}
$$

The third basic lemma is a pure ODE result, reaping the benefits of the other two.

Lemma 3 *(ODE)*
If $0 \leq \theta \leq 1$ and $r > 0$ satisfy (21), then $E\,L \gtrsim 1$ and $(\dot{L})^2 \lesssim -\dot{E}$ imply

$$
\fint_0^T E^{\theta r} L^{-(1-\theta)r}\, dt \;\gtrsim\; T^{-\frac{r}{3}} \quad \text{\itshape for} \quad T \gg L_0^3. \tag{24}
$$

If $0 \leq \theta \leq 1$ and $r > 0$ satisfy (22), then $E\,L \gtrsim 1$ and $(\dot{L})^2 \lesssim E\,(-\dot{E})$ imply

$$
\fint_0^T E^{\theta r} L^{-(1-\theta)r}\, dt \;\gtrsim\; T^{-\frac{r}{4}} \quad \text{\itshape for} \quad T \gg L_0^4. \tag{25}
$$

4.2 Proof of Lemma 1

We present the proof for the case of constant mobility. The argument for the case of degenerate mobility is similar (actually slightly easier, since when the mobility is degenerate we have $-1 \leq m \leq 1$).

The first ingredient is the well-known Modica-Mortola [22] inequality. Defining

$$
W(m) \;:=\; \int_0^m |1 - t^2|\, dt, \tag{26}
$$

we have

$$
\frac{\partial W}{\partial m} \;=\; |1 - m^2|,
$$

so

$$
\fint |\nabla(W(m))|\, dx \;=\; \fint |\nabla m|\frac{\partial W}{\partial m}\, dx \;\leq\; \fint \frac{1}{2}\left(|\nabla m|^2 + (\frac{\partial W}{\partial m})^2\right)\, dx \;=\; E. \tag{27}
$$

The second ingredient is the interpolation estimate

$$\fint m^2 \, dx \; \lesssim \; \left(\fint |\nabla(W(m))| \, dx \fint |\nabla^{-1}m| \, dx \right)^{\frac{1}{2}} + E \tag{28}$$

with $\fint |\nabla^{-1}m| \, dx = L$ defined by (20). The proof of (28) makes use of a smooth mollifier φ which is radially symmetric, non negative, and supported in the unit ball with $\int_{R^N} \varphi = 1$. Let the subscript ε denote the convolution with the kernel

$$\frac{1}{\varepsilon^N} \, \varphi(\frac{\cdot}{\varepsilon}).$$

We split the L^2-norm according to

$$\fint m^2 \, dx \; \lesssim \; \fint (m - m_\varepsilon)^2 \, dx + \fint m_\varepsilon^2 \, dx. \tag{29}$$

For the first term in (29), we observe that

$$(m_1 - m_2)^2 \; \lesssim \; |W(m_1) - W(m_2)|$$

as an easy consequence of the definition (26). Therefore

$$
\begin{aligned}
\fint (m - m_\varepsilon)^2 \, dx \;\; &\leq \;\; \sup_{|h| \leq \varepsilon} \fint (m(x) - m(x+h))^2 \, dx \\
&\lesssim \;\; \sup_{|h| \leq \varepsilon} \fint |W(m(x)) - W(m(x+h))| \, dx \\
&\lesssim \;\; \varepsilon \fint |\nabla(W(m))| \, dx. \tag{30}
\end{aligned}
$$

For the second term in (29), we must deal separately with large and small $|m_\varepsilon|$-values:

$$\fint m_\varepsilon^2 \, dx \; = \; \fint (m_\varepsilon^2 - \min\{m_\varepsilon^2, 4\}) \, dx + \fint \min\{m_\varepsilon^2, 4\} \, dx. \tag{31}$$

(The case of degenerate mobility is easier at this point, since $\sup |m_\varepsilon| \leq 1$.) To estimate the first term in (31) we observe that since $m^2 - \min\{m^2, 4\}$ is non-zero only for $|m| > 2$, we have the following pointwise estimate by the energy density

$$m^2 - \min\{m^2, 4\} \; \lesssim \; \frac{1}{2} \, (1 - m^2)^2. \tag{32}$$

Furthermore, $m^2 - \min\{m^2, 4\}$ is convex in m. Hence we obtain by Jensen's inequality

$$
\begin{aligned}
\fint (m_\varepsilon^2 - \min\{m_\varepsilon^2, 4\}) \, dx \;\; &\leq \;\; \fint (m^2 - \min\{m^2, 4\}) \, dx \\
&\overset{(32)}{\lesssim} \;\; \fint \frac{1}{2} \, (1 - m^2)^2 \, dx \; \leq \; E. \tag{33}
\end{aligned}
$$

To estimate the second term in (31), we observe that

$$\fint \min\{m_\varepsilon^2, 4\}\, dx \;\lesssim\; \fint |m_\varepsilon|\, dx. \tag{34}$$

Since the convolution operator is symmetric in the L^2 norm and

$$\sup |\nabla \zeta_\varepsilon| \;\lesssim\; \frac{1}{\varepsilon}\, \sup |\zeta| \quad \text{for any function } \zeta,$$

a duality argument gives

$$\fint |m_\varepsilon|\, dx \;\lesssim\; \frac{1}{\varepsilon}\, \fint |\nabla^{-1} m|\, dx. \tag{35}$$

Combining (30), (33), (34) and (35), we conclude that

$$\fint m^2\, dx \;\lesssim\; \varepsilon \fint |\nabla(W(m))|\, dx + \frac{1}{\varepsilon} \fint |\nabla^{-1} m|\, dx + E.$$

Optimization over ε gives the desired interpolation inequality (28).

The final ingredient is the elementary estimate

$$1 - \fint m^2\, dx \;=\; \fint (1 - m^2)\, dx \;\leq\; \left(\fint (1 - m^2)^2\, dx \right)^{1/2} \;\lesssim\; E^{1/2}.$$

Together with (27) and (28), we obtain as desired

$$1 \;\lesssim\; (E\, L)^{1/2} + E + E^{1/2},$$

which yields Lemma 1 for $E \ll 1$.

4.3   Proof of Lemma 2

In the constant mobility setting, the PDE (10) can be written as

$$\frac{\partial m}{\partial t} + \nabla \cdot J \;=\; 0 \quad \text{where} \quad J \;:=\; -\nabla \frac{\partial E}{\partial m}, \tag{36}$$

and its solutions are known to be classical. Therefore the rate of change of E is

$$-\dot{E} \;=\; -\fint \frac{\partial E}{\partial m}\, m_t\, dx = \fint |J|^2\, dx. \tag{37}$$

Concerning the rate of change of L, we claim that for any $t_1 < t_2$,

$$|L(t_2) - L(t_1)| \;\leq\; \int_{t_1}^{t_2} \fint |J|\, dx\, dt. \tag{38}$$

Indeed, let $\zeta_*(x)$ be an optimal test function in the definition of (20) of $L(t_2)$; thus

$$L(t_2) \;=\; \fint m(x, t_2)\, \zeta_*(x)\, dx$$

and ζ_* is periodic and Lipschitz continuous with $|\nabla\zeta_*| \leq 1$. Using ζ_* as a test function in the definition of $L(t_1)$ gives

$$
\begin{aligned}
L(t_2) - L(t_1) &\leq \fint (m(x,t_2) - m(x,t_1))\, \zeta_*\, dx \\
&= \int_{t_1}^{t_2} \fint \frac{\partial m}{\partial t}\, \zeta_*\, dx\, dt \\
&\overset{(36)}{=} \int_{t_1}^{t_2} \fint J\cdot\nabla\zeta_*\, dx\, dt \\
&\leq \int_{t_1}^{t_2} \fint |J|\, dx\, dt.
\end{aligned}
$$

The opposite inequality

$$
L(t_1) - L(t_2) \leq \int_{t_1}^{t_2} \fint |J|\, dx\, dt
$$

is proved similarly, choosing ζ_* to be optimal for the definition of $L(t_1)$. Thus (38) holds.

The conclusion of Lemma 2 follows easily from (37) and (38). Indeed, from the latter we see that L is an absolutely continuous function of t and

$$
|\dot{L}| \leq \fint |J|\, dx. \tag{39}
$$

Applying Cauchy-Schwarz inequality and using (37) we conclude that

$$
|\dot{L}| \leq \left(\fint |J|^2\, dx\right)^{1/2} = \left(-\dot{E}\right)^{1/2}
$$

which is the assertion of the Lemma in the constant mobility setting.

The proof in the degenerate mobility setting is very similar. The PDE in this case is (11), which can be written as

$$
\frac{\partial m}{\partial t} + \nabla\cdot J = 0 \quad \text{where} \quad J := -(1-m^2)\nabla\frac{\partial E}{\partial m}. \tag{40}
$$

For a classical solution, (40) implies

$$
-\dot{E} = \fint \frac{1}{1-m^2}|J|^2\, dx. \tag{41}
$$

The variation of L is still estimated by (39), and the Cauchy-Schwarz inequality gives

$$
\fint |J|\, dx \leq \left(\fint \frac{1}{1-m^2}|J|^2\, dx \fint (1-m^2)\, dx\right)^{\frac{1}{2}}. \tag{42}
$$

We also have

$$
E \geq \fint \frac{1}{2}(1-m^2)\, dx. \tag{43}
$$

Combining inequalities (39), (41), (42) and (43) we conclude that

$$(\dot{L})^2 \ \leq \ -2E\dot{E}, \tag{44}$$

which is the assertion of Lemma 2 in the degenerate mobility setting.

It is not known whether the degenerate-mobility Cahn-Hilliard equation (40) has a global-in-time classical solution. However Elliott & Garcke proved the existence of a global-in-time weak solution in [9], and the argument just presented extends to the weak solutions constructed by those authors. Indeed, their solutions are obtained by a limiting procedure involving Cahn-Hilliard equations similar to (40), but with a finite quench (so the energy is (5) with $\beta > 0$) and regularized mobility. The regularized equations have classical solutions and support estimates analogous to (41)-(43). There is sufficient compactness to pass to the limit in L and E, and the analogues of (41) give in the limit the energy *inequality*

$$-\dot{E} \ \geq \ \fint \frac{1}{1-m^2} \, |J|^2 \, dx$$

(the situation is analogous to Leray-Hopf weak solutions of the Navier-Stokes equations). This is, fortunately, all we really needed from (41): passing to the limit in the regularized version of

$$|\dot{L}| \ \leq \ \left(\fint \frac{1}{1-m^2} \, |J|^2 \, dx \fint (1-m^2) \, dx \right)^{\frac{1}{2}},$$

and noting that $-2E\dot{E} = -dE^2/dt$ we conclude that for the limiting weak solution L is absolutely continuous, $-dE^2/dt$ is a bounded measure, and

$$(\dot{L})^2 \ \leq \ -2dE^2/dt.$$

This is the sense in which the dissipation relation holds for weak solutions.

4.4   Proof of Lemma 3

We begin with some remarks, showing that Lemma 3 takes more or less optimal advantage of its hypotheses. Let us focus for simplicity on the case of constant mobility.

Remark 2 *We shall prove a weak form of the statement $E \gtrsim t^{-1/3}$, but we cannot expect to prove any form of the analogous-looking statement $L \lesssim t^{1/3}$.*

Indeed, the hypotheses $E\,L \ \gtrsim \ 1$ and $(\dot{L})^2 \ \lesssim \ -\dot{E}$ are consistent with the choice

$$L \ := \ t^\alpha \quad \text{and} \quad E \ := \ t^{-\beta}$$

provided

$$0 \ \leq \ \beta \ \leq \ \alpha \quad \text{and} \quad \beta \ \leq \ 1 - 2\,\alpha. \tag{45}$$

These inequalities imply that $\beta \leq 1/3$, consistent with the expected result $E \gtrsim t^{-1/3}$. However they permit α to take any value between 0 and $1/2$. Thus our approach cannot give an upper bound on L better than $L \lesssim t^{1/2}$.

Remark 3 *Extending the preceding comment: we can expect to prove a weak form of the statement $E^\theta L^{-(1-\theta)} \gtrsim t^{-1/3}$ only for $1/3 \leq \theta \leq 1$.*

Indeed, it is easy to see that

$$0 \leq \beta \leq \alpha \quad \text{and} \quad \beta \leq 1 - 2\alpha \quad \text{imply} \quad \theta\beta + (1-\theta)\alpha \leq 1/3$$

only if $1/3 \leq \theta \leq 1$.

Remark 4 *Our tools are not sufficient to prove a* pointwise *version of the statement $E \gtrsim t^{-1/3}$.*

Indeed, for any $0 < E_1 \ll 1$, consider the functions

$$E(t) := 1 - E_1^2 t \quad \text{and} \quad L(t) := 1 + E_1 t.$$

They satisfy the restrictions $\dot{E} \leq 0$ and $(\dot{L})^2 \lesssim -\dot{E}$ trivially, and they also satisfy $E L \gtrsim 1$ on the finite time horizon

$$t \leq t_1 := \frac{1 - E_1}{E_1^2} \approx \frac{1}{E_1^2}.$$

Since

$$E(t_1) = E_1,$$

this example rules out any pointwise lower bound of the form

$$E(t) \gtrsim t^{-\gamma} \quad \text{with} \quad \gamma < \frac{1}{2}.$$

We now begin the proof of Lemma 3. We present the argument just for the case of degenerate mobility; the other case, when the mobility is constant, is entirely similar. We may assume $E(t)$ and $L(t)$ are differentiable since the hypotheses $E L \gtrsim 1$ and $(\dot{L})^2 \lesssim -d(E^2)/dt$ are preserved under mollification.

The differential inequality $(\dot{L})^2 \lesssim E(-\dot{E})$ implies that E is a monotone function of time, and L is an absolutely continuous function of E. Therefore L can be viewed as a function of E, and the differential inequality can be rewritten as

$$\left(\frac{dL}{de}\right)^2 (\dot{E})^2 \lesssim E|\dot{E}|.$$

Here we use the lower case e for the energy as an independent variable to distinguish it from $E = E(t)$. Division by $E|\dot{E}| \geq 0$ gives

$$\frac{1}{E}\left(\frac{dL}{de}\right)^2 |\dot{E}| \lesssim 1. \tag{46}$$

(The division is inadmissible if $\dot{E} = 0$, but the conclusion (46) is trivial in that case, so this conclusion is valid for all $t > 0$.) Multiplying by any function $f(E(t))$ and integrating in time gives

$$\int_0^T f(E(t))dt \gtrsim \int_{E(T)}^{E(0)} \frac{f(e)}{e}\left(\frac{dL}{de}\right)^2 de.$$

Taking $f = e^{\theta r}L^{-(1-\theta)r}$ and writing $E_0 = E(0)$, $E_T = E(T)$, we reach the conclusion that

$$\int_0^T E^{\theta r}(t)\, L^{-(1-\theta)r}(t)dt \;\gtrsim\; \int_{E_T}^{E_0} e^{\theta r - 1}L^{-(1-\theta)r}\left(\frac{dL}{de}\right)^2 de \tag{47}$$

for all $T > 0$.

Now we must estimate the right hand side of (47). Consider the change of variables

$$\hat{e} \;=\; \frac{1}{2-\theta r}\, e^{2-\theta r}, \quad \text{and} \quad \hat{L} \;=\; \frac{1}{1-\frac{(1-\theta)r}{2}}\, L^{1-\frac{(1-\theta)r}{2}}.$$

Our hypotheses

$$\theta\, r > 2, \quad (1-\theta)\, r < 2 \tag{48}$$

assure that $\hat{e} \to \infty$ and $\hat{L} \to \infty$ as $e \to 0$ and $L \to \infty$ respectively. They also imply

$$\theta > 1/2, \tag{49}$$

which will be needed below. Since

$$\left(\frac{dL}{de}\right)^2 de = \left(\frac{d\hat{L}}{d\hat{e}}\right)^2 \left(\frac{dL}{d\hat{L}}\right)^2 \left(\frac{d\hat{e}}{de}\right) d\hat{e}$$

we have

$$\int_{E_T}^{E_0} e^{\theta r - 1}L^{-(1-\theta)r}\left(\frac{dL}{de}\right)^2 de \;=\; \int_{\hat{E}_0}^{\hat{E}_T}\left(\frac{d\hat{L}}{d\hat{e}}\right)^2 d\hat{e}.$$

The right hand side is bounded below by the minimum over all functions $\hat{L}(\hat{e})$ with the same end conditions

$$\hat{L}(\hat{E}_0) = \frac{1}{1-\frac{(1-\theta)r}{2}}(L(0))^{1-\frac{(1-\theta)r}{2}}, \quad \hat{L}(\hat{E}_T) = \frac{1}{1-\frac{(1-\theta)r}{2}}(L(T))^{1-\frac{(1-\theta)r}{2}}.$$

To simplify notation we denote these end conditions by $\hat{L}_0$ and $\hat{L}_T$ respectively. The extremal $\hat{L}$ is of course linear in $\hat{e}$, so we have

$$\int_0^T E^{\theta r}(t)L^{-(1-\theta)}(t)dt \;\gtrsim\; \frac{\left(\hat{L}_T - \hat{L}_0\right)^2}{\hat{E}_T - \hat{E}_0}. \tag{50}$$

When T is such that
$$L(T) \geq 2L(0)$$
the right side of (50) is easy to control: we have
$$\hat{L}_T - \hat{L}_0 \gtrsim \hat{L}_T \quad \text{and} \quad \hat{E}_T - \hat{E}_0 \leq \hat{E}_T$$
so
$$\int_0^T E^{\theta r} L^{-(1-\theta)r}\, dt \ \gtrsim\ \frac{\hat{L}_T^2}{\hat{E}_T}\ =\ L_T^{2-(1-\theta)r} E_T^{\theta r - 2}.$$
Rewriting the right hand side as
$$L_T^{2-(1-\theta)r} E_T^{\theta r - 2} = [E_T^\theta L_T^{-(1-\theta)}]^{r-4}\, [L_T E_T]^{4\theta - 2}$$
we conclude, using $EL \gtrsim 1$ and (49), that
$$\int_0^T E^{\theta r} L^{-(1-\theta)r}\, dt \ \gtrsim\ [E_T^\theta L_T^{-(1-\theta)}]^{r-4} \quad \text{provided } L(T) \geq 2L(0). \qquad (51)$$
Introducing
$$h(T) \ := \ \int_0^T E^{\theta r} L^{-(1-\theta)r}\, dt,$$
we can rewrite (51) as $h \gtrsim (h')^{(r-4)/r}$, so we have shown that
$$h^{r/(4-r)}(T) h'(T) \gtrsim 1 \quad \text{provided } L(T) \geq 2L(0). \qquad (52)$$
Here, we have used $r < 4$.

The preceding method doesn't work when $L(T) < 2L(0)$, but for such T we can estimate $h'(T) = E^{\theta r}(T) L^{-(1-\theta)r}(T)$ by different, more elementary means. Indeed, for such T we have
$$E(T) \gtrsim L^{-1}(T) \gtrsim L_0^{-1},$$
which implies
$$E^\theta(T) L^{-(1-\theta)}(T) \gtrsim L_0^{-1}.$$
Thus
$$h'(T) \gtrsim L_0^{-r} \quad \text{if } L(T) < 2L_0. \qquad (53)$$
Combining (52) and (53) we conclude, using $r < 4$, that
$$\frac{d}{dt}\left(h + L_0^{4-r}\right)^{\frac{4}{4-r}} \sim \left(h(t) + L_0^{4-r}\right)^{\frac{r}{4-r}} h'(t) \gtrsim 1 \quad \text{for all } t > 0.$$
Integration in time gives
$$h(T) + L_0^{4-r} \gtrsim T^{\frac{4-r}{4}} \quad \text{for all } T > 0.$$
Restricting attention to $T \gg L_0^4$, this becomes
$$\int_0^T E^{\theta r} L^{-(1-\theta)r}\, dt = h(T) \gtrsim T^{\frac{4-r}{4}} \quad \text{for } T \gg L_0^4,$$
which is precisely the conclusion of Lemma 3.

5 Discussion

We explained in Section 1 that upper bounds on coarsening rates are different from lower bounds, because upper bounds are kinematic and universal, while lower bounds are geometry-dependent. Our rigorous results demonstrate the merit of this viewpoint, by using simple dissipation and interpolation relations to prove weak, time-averaged upper bounds.

It would be nice to prove more. We suppose E and L should satisfy pointwise-in-time bounds. But proving this seems to require a new idea, if not an entirely new method.

This paper addresses just two of the many energy-driven coarsening models in materials science. Other examples include the coarsening of mounds in epitaxial growth (see e.g. [23, 29, 30]) and the coarsening of defect structures in soft condensed matter (see e.g. [17]). We wonder whether the viewpoint and methods of this paper might be applicable to such problems.

References

[1] N. Alikakos, P. Bates, X. Chen, Convergence of the Cahn-Hilliard equation to the Hele-Shaw model, *Arch. Rat. Mech. Anal.* **128** (1994), 165–205

[2] L. Bronsard, H. Garcke, B. Stoth, A multi-phase Mullins-Sekerka systems: matched asymptotic expansions and an implicit time discretizations for the geometric evolution problems, *Proc. Royal Soc. Edinburgh Ser. A* **128** (1998), 481–506

[3] J. W. Cahn, C. M. Elliott, A. Novick-Cohen, The Cahn-Hilliard equation with a concentration dependent mobility: motion by minus the Laplacian of the mean curvature, *European J. Appl. Math.* **7** (1996), 287–301

[4] X. Chen, Global asymptotic limit of solutions of the Cahn-Hilliard equation, *J. Diff. Geom.* **44** (1996), 262–311

[5] R. Choksi, R. V. Kohn, F. Otto, Domain branching in uniaxial ferromagnetics: a scaling law for the minimum energy, *Commun. Math. Phys.* **201** (1999), 61–79

[6] A. Cohen, R. DeVore, P. Petrushev, H. Xu, Nonlinear approximation and the space $BV(R^2)$, *Amer. J. Math.* **121** (1999), 587–628

[7] A. Cohen, Y. Meyer, F. Oru, An improved Sobolev inequality, *Proc. Séminaires X-EDP* No. IV, Centre de Math., Ecole Polytechnique, Palaiseau, France (1998)

[8] P. Constantin, C. R. Doering, Infinite Prandtl number convection. *J. Stat. Phys.* **94** (1999), 159–172

[9] C. M. Elliott, H. Garcke, On the Cahn-Hilliard equation with degenerate mobility, *SIAM J. Math. Anal.* **27** (1996), 404–423

[10] P. C. Fife, Models for phase separation and their mathematics, *Electron. J. Diff. Eqns.* **2000** (2000), No. 48, 1–26

[11] P. Fratzl, J. L. Lebowitz, Universality of scaled structure functions in quenched systems undergoing phase-separation, *Acta Metall.* **37** (1989), 3245–3248

[12] P. Fratzl, J. L. Lebowitz, O. Penrose, J. Amar, Scaling functions, self-similarity, and the morphology of phase separating systems, *Phys. Rev. B* **44** (1991), 4794–4811

[13] H. Garcke, A. Novick-Cohen, A singular limit for a system of degenerate Cahn-Hilliard equations, *Adv. in Diff. Equations* **5** (2000), 401–434

[14] G. Giacomin, J. L. Lebowitz, E. Presutti, Deterministic and stochastic hydrodynamic equations arising from simple microscopic model systems, in R. A. Carmona & B. Rozovskii eds., *Stochastic Partial Differential Equations: Six Perspectives*, Math. Surveys and Monographs **44**, American Mathematical Society (1997), 107–152

[15] G. Giacomin, J. L. Lebowitz, Phase segregation dynamics in particle systems with long range interactions II: Interface motion, *SIAM J. Appl. Math.* **58** (1998), 1707–1729

[16] Y. Giga and R. V. Kohn, Asymptotically self-similar blowup of semilinear heat equations, *Comm. Pure Appl. Math.* **38** (1985), 297–319

[17] C. Harrison, D. H. Adamson, Z. D. Cheng, J. M. Sebastian, S. Sethuraman, D. A. Huse, R. A. Register, and P. M. Chaikin, Mechanisms of ordering in striped patterns, *Science* **290** (2000) 5497:1558–1560

[18] T. Hashimoto, M. Itakura, N. Shimidzu, Late stage spinodal decomposition of a binary polymer mixture. II. Scaling analyses on $Q_m(\tau)$ and $I_m(\tau)$, *J. Chem. Phys.* **85** (1986), 6773–6786

[19] M. A. Herrero and J. J. L. Velazquez, Explosion de solutions d'équations paraboliques semilinéaires supercritiques, *C. R. Acad. Sci. Paris Sér. I Math.* **319** (1994) no. 2, 141–145.

[20] T. Izumitani, M. Tanenaka, T. Hashimoto, Late stage spinodal decomposition of a binary polymer mixture. III. Scaling analyses of late-stage unmixing, *J. Chem. Phys.* **92** (1990), 3213–3221

[21] I. M. Lifshitz, V. V. Slyozov, The kinetics of precipitation from supersaturated solid solutions, *J. Phys. Chem. Solids* **19** (1961), 35–50

[22] L. Modica, S. Mortola, Un esempio di Γ-convergenza, *Boll. U.M.I* **14** (1977), 285–299

[23] D. Moldovan, L. Golubovic, Interfacial coarsening dynamics in epitaxial growth with slope selection, *Phys. Rev. E* **61** (2000), 6190–6214

[24] B. Niethammer, Derivation of the LSW-theory for Ostwald ripening by homogenization methods, *Archive Rat. Mech. Anal.* **147 (2)** (1999), 119–178

[25] B. Niethammer, F. Otto, Ostwald ripening, The screening length revisited, *Calc. Var.* **13** (2001), 33–68.

[26] B. Niethammer, R. Pego, Non-self-similar behavior in the LSW theory of Ostwald ripening, *J. Stat. Phys.* **95** (1999), 867–902

[27] R. Pego, Front migration in the nonlinear Cahn-Hilliard equation, *Proc. Royal Soc. London A* **422** (1989), 261–278

[28] S. Puri A. J. Bray, & J. L. Lebowitz, Phase-separation kinetics in a model with order-parameter-dependent mobility, *Phys. Rev. E* **56** (1997), 758–765

[29] M. Ortiz, E. Repetto, & H. Si, A continuum model of kinetic roughening and coarsening in thin films, *J. Mech. Phys. Solids* **47** (1999), 697–730

[30] M. Siegert, Ordering dynamics of surfaces in molecular beam epitaxy, *Physica A* **239** (1997) 420–427

[31] C. Wagner, Theorie der Alterung von Niederschlägen durch Umlösen, *Z. Elektrochemie* **65** (1961), 581–594